Experimental investigation of a PVC geomembrane response to different tensile loading modes

Nesrin Akel[1*], *Laurent* Josseaume[1], *Guillaume* Stoltz[1], *Antoine* Wautier[1], *Nathalie* Touze[2] and *François* Nicot[3]

[1] INRAE, Aix Marseille Univ, RECOVER, Aix-en-Provence, France
[2] Université Paris-Saclay, INRAE, SDAR, Jouy-en-Josas, France
[3] Université Savoie Mont-Blanc, ISTerre, Le Bourget-du-Lac, France

Abstract. Geomembrane are not meant to support mechanical actions, however, one of the main causes of the malfunctioning of their waterproofing properties is attributed to the unexpected tensile forces that may be generated during its service life, and that may potentially lead to failure. Driven by this meticulous problem, this study focuses on characterizing the tensile behaviour of Polyvinyl Chloride geomembranes by evaluating their failure criteria in terms of resistance and elongation. A wide range of tensile loading rates was applied to investigate the rate-dependent effects on the material's ultimate properties. Additionally, complementary long-term (creep) tests were conducted to examine the impact of the loading weight on the failure thresholds. Based on these results, this study proves that creep behaviour can be predicted through tensile tests, provided the environmental conditions remain constant. The results highlight the important role of the loading rates on the GM performance, providing a solid base for engineering design.

1 Introduction

Geomembranes, a particular type of geosynthetics, play an important function as barriers to limit fluid migration. In the last decade, it is considered as an important tool that contributes in the sustainable development and resource management [1,2].

Driven by its remarkable flexibility and deformability, Polyvinyl chloride (PVC) geomembrane (GM) is one of the most used GMs in dams and canals [3]. Although it is not designed to support mechanical actions, it may experience unexpected internal tensile forces during installation (e.g., in-situ casting, placement of concrete blocks or even soil, improper installation, operational problems), or along its service life (e.g., earthquakes, contact with angular solids, wind actions, weakening of the subgrade). This results in various severe consequences ranging from loss of stored fluid to structural failure [4,5]. Thus, beside its waterproofing properties, the mechanical properties of geomembrane are essential considerations for engineers when designing waterproofing systems.

* Corresponding author: nesrin.akel@inrae.fr

© The Authors, published by EDP Sciences. This is an open access article distributed under the terms of the Creative Commons Attribution License 4.0 (https://creativecommons.org/licenses/by/4.0/).

Engineers typically rely on short-term laboratory tests to design waterproofing systems during the entire service life. Uniaxial tensile tests, being the most straightforward experimental approach, are used for the determination of the mechanical properties of materials in terms of their stress-strain behaviour. The European standard EN12311 [6], for instance, specifies a tensile rate of 100 mm/min when conducting a uniaxial tensile test, that may not accurately reflect in-situ scenarios. Therefore, it is of the key importance to study how the distribution of forces (i.e., the loading rate) affects the PVC GM's mechanical properties [7] , in order to help engineers to better predict and assess the GM behaviour.

To address this inquiry, this study investigates how these forces affects the tensile strength and elongation at failure on the short- and long-term by evaluating the rate-dependent effect. Uniaxial tensile tests are conducted over a wide range of tensile rates, from 0.01 to 500 mm/min. Additionally, creep tests are performed under varying loading weights to assess their impact on creep behaviour and to determine the ultimate properties and long-term failure criteria.

The results from these tests help engineers to securely design a waterproofing system using PVC GM, by providing a complementary comprehensive analysis, offering critical insights into its performance under different loading conditions.

2 Materials and Methodology

2.1 Materials and specimens preparation

The geomembrane type used in this study was carefully selected to mitigate the impact of additives, including antioxidants, fillers, carbon black, and fire retardants on the integrity of the research outcomes.

Throughout the entire experimental campaign, a transparent Polyvinyl Chloride (PVC) geomembrane with a thickness of 3 mm was employed, composed of PVC resin, plasticizer, and stabilizer. This formulation was specifically designed for a tunnel project.

By adopting such a composition, the choice facilitates a more rigorous evaluation of the fundamental properties of PVC geomembranes, ensuring that the findings are faithfully unaffected by the presence of additives.

Specimens were randomly extracted from a roll of PVC geomembrane, and cut into dumbbell-shaped specimens using a standardised cutter, with dimensions conform to the European standard specification EN12311 (Method B) [6].

Two marker reference points were placed on the specimen's less bright side using a template. These points were considered to measure the relative longitudinal elongation of the specimen.

2.2 Apparatus and testing procedure

Two types of tests were conducted in this study: short-term tests via uniaxial tensile testing and long-term tests through creep testing. All tests were performed at a controlled temperature of 23 ± 2 °C and a relative humidity ranging from 30% to 70%.

2.2.1 Uniaxial tensile test

Examining the impact of rate dependency on the tensile strength and strain at failure is of paramount importance, as it is essential for accurately assessing the material's resistance and

elongation before failure, thereby informing engineering design decisions for hydraulic projects.

The test setup comprises a tensile testing machine equipped with upper and lower grips for holding the specimen, and a force sensor with a sufficient loading capacity (at least 2000 N), as shown in **Fig.*1***. The clear distance between the grips is set at 80 mm, according to the same standard.

The testing procedure involves subjecting a PVC GM specimen to continuous stretching at a constant displacement rate. A video extensometer is employed to measure the relative displacement between two predefined markers on the specimen. Concurrently, an acquisition system continuously records both the tensile force and the corresponding longitudinal relative displacement in the specimen. The test ends when the failure occurs.

According to the European standard EN12311 (AFNOR 2013) [6], which specifies methods for determining the tensile properties of plastic and rubber sheets, a speed of 100 mm/min is recommended. However, in this study, a wide range of displacement rate has been employed, spanning from 0.01 to 500 mm/min. For each tensile speed, at least three repeatability tests have been carried out. This range of displacement rates allows for a comprehensive understanding of the material's response to different loading conditions.

The outcome of this test is a force-strain curve, wherein the strain represents the engineering strain (i.e., infinitesimal strain) expressed as the ratio of the incremental length to the initial length **Eq.1**.

$$\varepsilon_{aE} = \frac{\Delta L}{L_0} = \frac{L_f - L_0}{L_0} \tag{1}$$

where ε_{aE} is the axial engineering strain or infinitesimal strain, L_0 is the initial relative length between the two predefined marked points on the specimen, and L_f is the final distance between them.

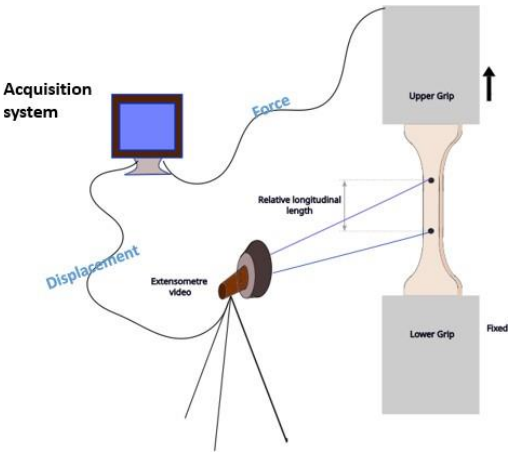

Fig.1. Uniaxial tensile test setup.

2.2.2 Creep test

Investigations through creep tests aim to evaluate the long-term characteristics of materials under constant stress. This is particularly important in engineering, as it significantly influences the design and selection of geomembrane. These tests are designed to evaluate rate dependency at slow tensile rates over extended periods.

The setup consists of a newly installed fixed frame that securely holds the geomembrane specimen. Two holes have been created in the non-homogeneous section part of the specimen. The upper part of the specimen is tightly anchored using a screw and a washer that fix it on the frame during testing. In the lower part, a hook is secured to the specimen as seen in **Fig.*2***. This hook connects to a rod that has a wooden platform for imposing the weight. A constant load is then applied by suspending weights gradually on the platform, exerting a constant uniaxial tensile force.

To measure the deformation over time, the relative displacement between the two marked points on the specimen is measured using a caliper. Additionally, a camera is set up in front of the test bench in order to accurately catch the exact time of specimen's failure.

A series of creep tests were conducted at various load levels (100, 110, 120, 140, 150, 200, 250 N) to examine the creep characteristics of the geomembrane under uniaxial tensile stress. The result of these tests is an engineering strain-time curve, with strain defined as previously shown in ***Eq.1***.

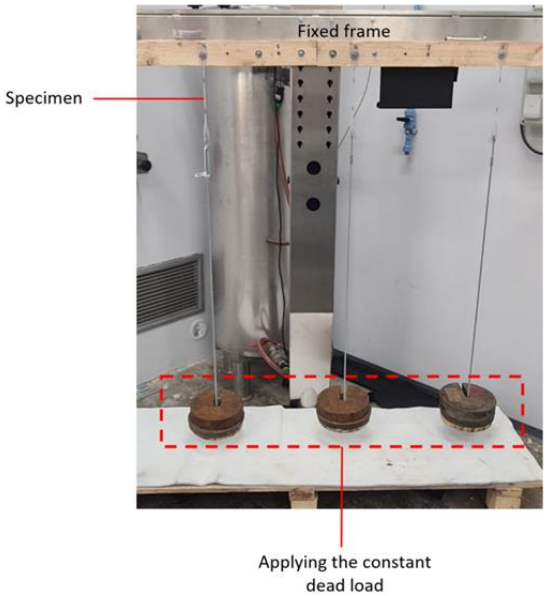

Fig.2. Creep Test Frame where several creep tests are conducted simultaneously.

3 Results

3.1 Short-term behaviour analysis

Fig.3 shows the force-engineering strain curves obtained from uniaxial tensile tests conducted at the specified aforementioned tensile rates. The recorded failure times span a range from approximately 20 seconds for the highest speed (500 mm/min) to nearly 11 days for the lowest speed (0.01 mm/min).

It can be shown that the relationship changes with applied uniaxial tensile rate. Notably, the material becomes more resistant at higher tensile rates, while concurrently exhibiting a more malleable behaviour at lower tensile rates.

Fig.4 shows the correlation between the maximum force resistance and engineering strain at failure with the tensile rate. It is evident that both the failure threshold in terms of material

resistance and elongation increase with higher tensile rates. As the tensile rate increases from 0.01 mm/min to 500 mm/min, the force at failure exhibits a significant upward linear trend in log scale, rising from approximately 150 N to 325 N (***Fig.4 (left)***). Similarly, the engineering strain at failure increases with higher loading rates, reaching around 390% at 500 mm/min. In contrast, at the lower loading rate of 0.01 mm/min, the material demonstrates an elongation of approximately 250% of its initial length (***Fig.4 (right)***).

Thus, the mechanical resistance and elongation at failure of PVC GM are considerably rate-dependent, pointing out the need of taking the loading rate into account during laboratory testing.

At high elongation rates (above 50 mm/min), the force at break appears to remain constant. While the exact cause is unclear, it may be related to material heterogeneity. Further repeatability testing and analysis are needed to confirm this hypothesis.

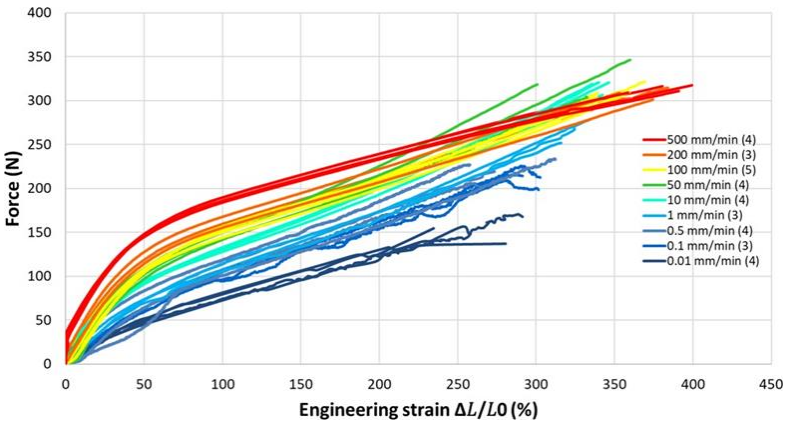

Fig.3. Force-engineering strain curves obtained from uniaxial tensile tests conducted at different tensile rates (mm/min). The values between brackets in the legend represent the number of repeatability tests conducted for each tensile speed.

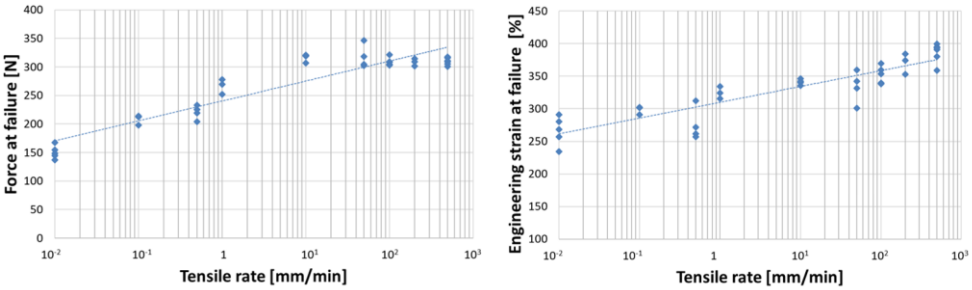

Fig.4. Variation of force and engineering strain at failure with tensile speed.

3.2 Creep behaviour analysis

The creep strain curves for testing the GM under various uniaxial tensile constant applied loads varied between 100 and 250 N and are displayed in ***Fig.5***.

Graphically, these curves are characterized by an instantaneous increase in stress, followed by a gradual decrease until a quasi-stable regime is reached, at which time the specimen splits (i.e., rupture under high loads).

Higher loads (200 N and higher) cause creep strain to grow quickly and quasi-stabilize more quickly, before failure occurs. The creep strain increases more gradually at intermediate loads (130 to 150 N), and it takes much longer (hours to days) for the strain to quasi-stabilize, followed by specimen's rupture. Lower loads (between 100 and 120 N) show a gradual raise in creep strain, taking days to months to reach a quasi-stable state.

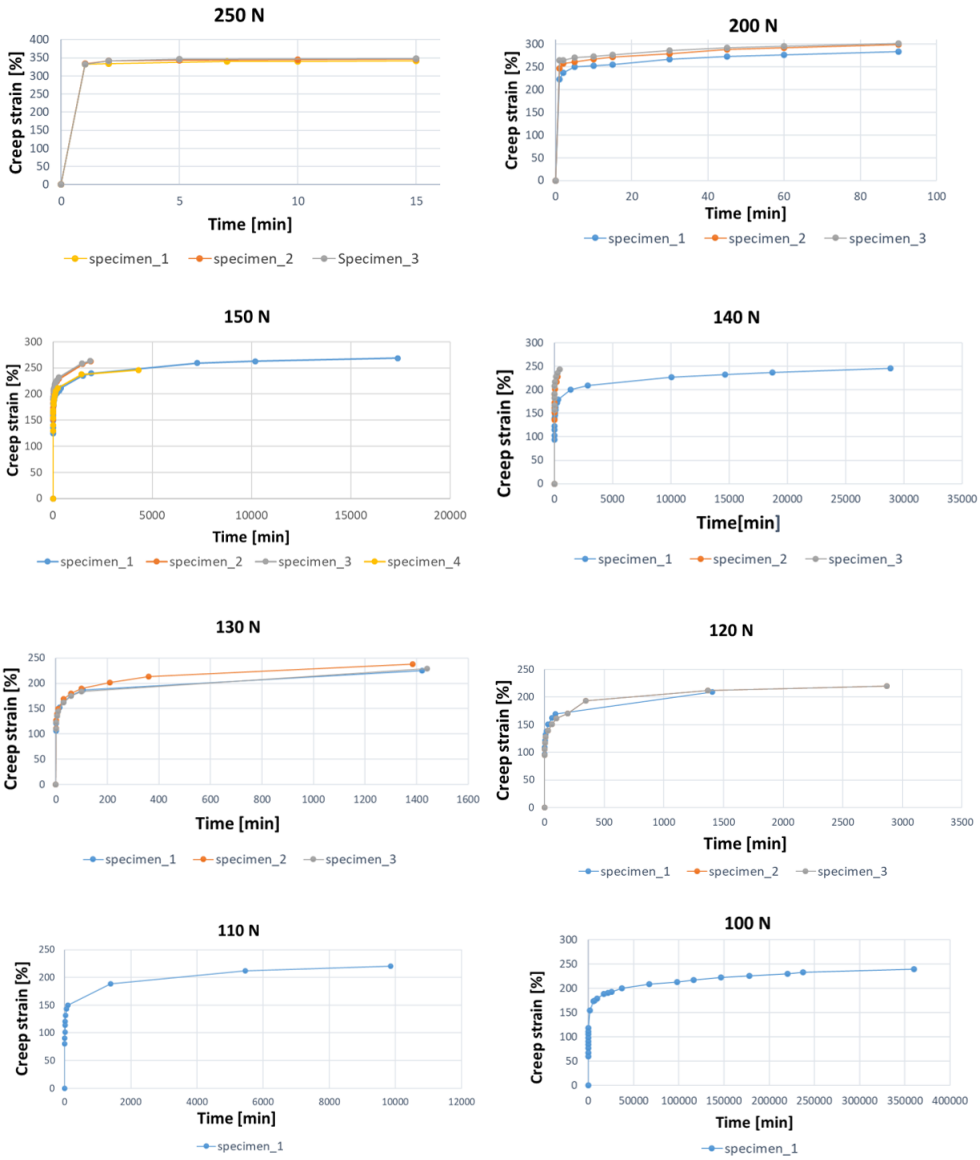

Fig.5. Creep strain curves at constant stresses of 250, 200, 150, 140, 130, 120, 110, and 100 N with the last point indicating failure. For the same loads, the results show variability due to material heterogeneity.

Fig.6 shows the time required for PVC specimens to fail under different constant loads. The results reveal that the failure time varies even with the same load, most likely due to the material's heterogeneity, which influences its behaviour. Additionally, the creep time to

rupture decreases as the load increases, indicating a direct correlation between the applied load and the rate at which the material approaches failure.

Fig.7 presents the creep strain observed at failure under different loading weights. The graph illustrates a linear tendency between the applied force and the creep strain at failure. Thus, the load at which the specimen splits (i.e., rupture of specimen) can be linked to the strain observed at failure.

Consequently, as shown in ***Fig.6*** and ***Fig.7***, the GM displays significant creep behaviour under different tensile loads, with higher loads resulting in both larger strain and a faster strain rate.

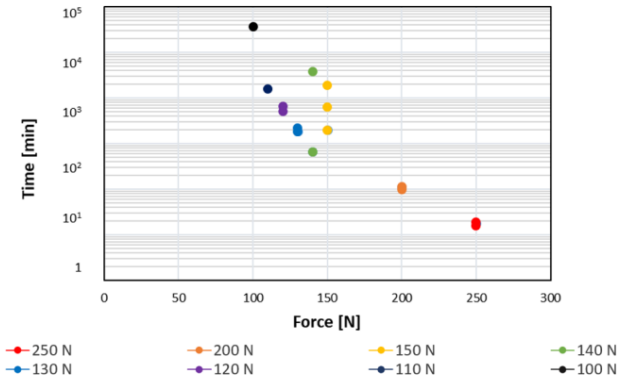

Fig.6. Creep failure time at different applied constant stresses.

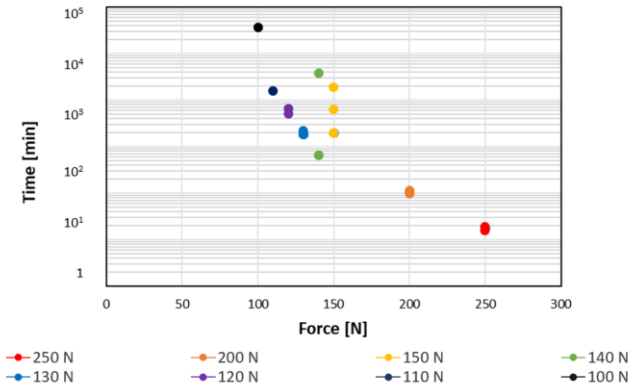

Fig.7. Strain at failure at different applied constant stresses.

A logarithmic scale offers a more effective representation of creep behaviour, as shown in ***Fig.8***, where a consistent linear creep strain is typically observed over time in a log scale. Additionally, it reveals that, even at a slower applied load (100N), the material continues to deform at a slower rate without entirely reaching a plateau.

For a deeper analysis of creep behaviour, the Sherby and Dorn [8] plot serves as a valuable tool to identify the different stages of creep. This plot presents the creep strain rate against the creep strain on a logarithmic scale, offering a clear view of how the creep rate evolves as strain increases. According to [9], geosynthetics creep behaviour can be divided into four distinct stages.

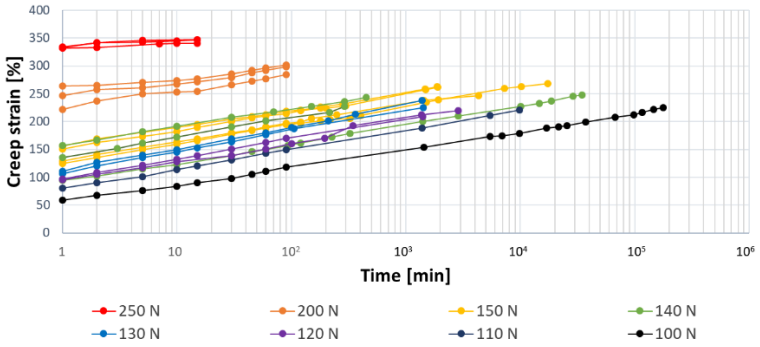

Fig.8. Creep strain curves at different applied constant stresses in logarithmic time scale.

The initial phase, namely instantaneous strain stage, occurs immediately upon the application of the load. This is followed by primary creep strain stage, which is characterized by a decreasing creep strain rate with increasing creep strain. Next comes the secondary creep stage, where the creep rate becomes constant or steady. Finally, in the tertiary creep stage, there is a rapid rise in creep strain, leading to material failure.

By analyzing ***Fig.9***, it can be observed that at higher loads (250-200N), the creep strain rate decreases rapidly, indicating an instantaneous deformation followed by specimens split (i.e., failure) without significant creep behaviour.

As the applied load decreases (150N and below), the primary stage is detected, and its duration lengthens, highlighted by a larger period of gradual reduction in the strain rate. Interestingly, the steady-state stage (*i.e., secondary creep stage*) and the tertiary creep stage could not be detected. These stages might be absent, suggesting that the material only exhibits primary creep stage at lower stresses.

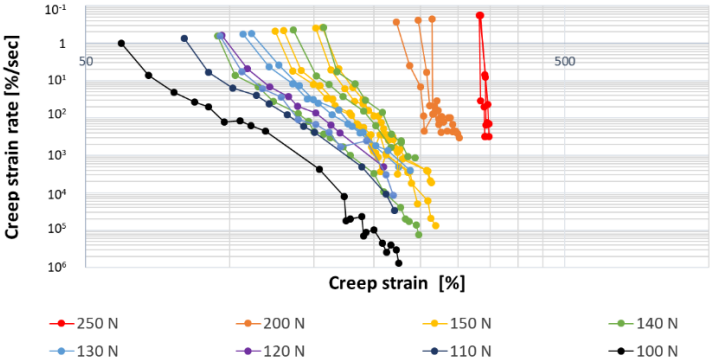

Fig. 9. Creep strain rate vs. creep strain.

4 Discussion

Based on these complementary results, a question about the intrinsic failure properties of the material—whether the failure criterion is primarily strain-based, stress-based, or a combination of both —is raised.

In order to address this inquiry, ***Fig. 7*** shows that when a creep load of 250 N is applied rapidly (from 0 to 250 N), the material fails at approximately 350% strain. The equivalent strain rate, calculated by dividing the strain at failure by the time to failure, was found to be

around 5 mm/min. When compared to the force-strain curves from **Fig.4**, we observe that at a tensile speed of 1 mm/min, which is of a similar magnitude to the equivalent creep strain rate (5 mm/min), the stress at failure ranged between 250 and 270 N, with corresponding strains between 300% and 350%. In the same way, ***Fig.10*** illustrates the force and engineering strain at failure corresponding to each tensile rate from tensile tests (conducted at constant tensile rate) and creep tests. Interestingly, the results reveal a good match between tests, implying that the material's creep performance (i.e., strength and strain) may be predictable based on its response via tensile tests at constant loading rate, at the same environmental conditions. Additionally, a very low tensile rate (10^{-5}) is achieved through creep test.

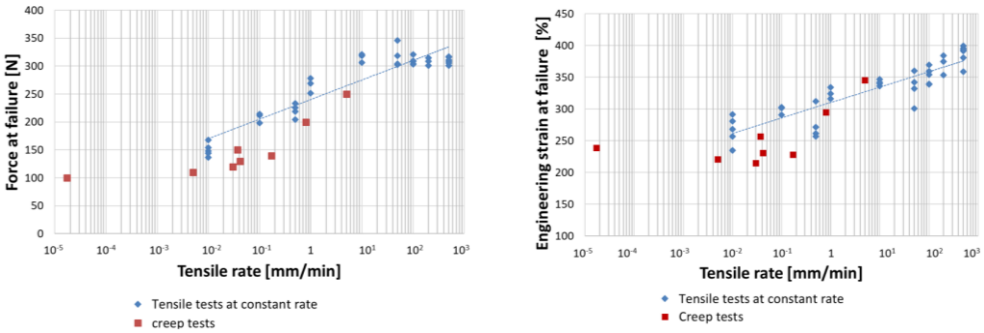

Fig.10. Force and engineering strain at failure for each tensile rate in long- and short-term testing.

The fact that failure occurs at consistent stress and strain values across both creep and uniaxial tensile tests suggests that the material's failure is not governed purely by exceeding a particular stress (a purely stress-based criterion) or strain threshold (a purely strain-based criterion). Instead, the strength and the strain at failure decrease when decreasing the loading rate. This indicates that the failure criteria cannot be easily defined where the effect of the viscosity persist even at very slow loading rates. Further repeatability tests at low tensile rates are required to more precisely refine the results.

5 Conclusion

This research aims to understand the PVC GM's response to unexpected tensile forces that may arise under various scenario, which presents challenges for engineers when designing waterproofing systems.

The study reveals that the material under study exhibits a rate-dependent behaviour, where higher loading rates leads to an increase in the resistance and elongation at failure.

Creep test results at high loads indicate that greater loads result in greater strain at failure and larger strain rate. This implies a strong correlation between the applied stress and the strain at which failure occurs.

Based on these complementary results, this study proves that the creep properties can be predicted by the tensile tests conducted at constant loading rate, provided the same environmental conditions (i.e., constant temperature, not exposed to UV radiation and humidity). Additionally, it has been proven that the effect of viscosity on failure properties (i.e., strength and stress at failure) persists even under very slow loading rates. Typically, the failure threshold in terms of strength and strain increases with higher loading rates.

From an engineering safety perspective, relatively short-term laboratory tests intended to predict the resistance of PVC GMs should be conducted at the lower rates expected in the field. This is important due to the impacts of rate dependency, which requires correct

measurements of intrinsic ultimate strength and deformation to reduce the risk of premature failure. Relying exclusively on tests conducted at 100 mm/min, as per the European standard EN12311, is not conservative, given that failures occurred sooner at lower speeds.

The results discussed in this research are specific to the GM being studied and should be extended carefully to other types of GMs in which other additives (such as antioxidants, fillers, carbon black, and fire retardants) may influence the mechanical behaviour as well.

Acknowledgments

This work is supported by the National Research Institute for Agriculture, Food and the Environment (INRAE) and by French Région Sud Provence-Alpes-Côte d'Azur (PACA), in addition an operating budget is provided by the industrial partner EGC Galopin.

References

1. N. Dixon, G. Fowmes, M. Frost, Global Challenges, Geosynthetic Solutions and Counting Carbon. Geosynthetics International 2017, 24, 451–464, doi:10.1680/jgein.17.00014.
2. N. Touze, Healing the World: A Geosynthetics Solution. *Geosynthetics International* **2020**, 1–31, doi:10.1680/jgein.20.00023.
3. D. Cazzuffi, D. Gioffrè, Geomembrane Barrier Systems for Construction and Rehabilitation of Embankment Dams. In; 2023; pp. 164–179 ISBN 978-1-00-329912-7.
4. A. Luciani, D. Peila, Tunnel Waterproofing: Available Technologies and Evaluation Through Risk Analysis. Int J Civ Eng 2019, 17, 45–59, doi:10.1007/s40999-018-0328-6.
5. R.K. Rowe, M.S. Ewais, A.M.R. Representative Stress Crack Resistance of Polyolefin Geomembranes Used in Waste Management. Waste Management 2019, 100, 18–27, doi:10.1016/j.wasman.2019.08.028.
6. AFNOR NF EN 12311-2. Flexible Sheets for Waterproofing - Determination of Tensile Properties - Part 2 : Plastic and Rubber Sheets for Roof Waterproofing. *Afnor EDITIONS* 2013.
7. S.M. Merry, J.D. Bray, Time-Dependent Mechanical Response of HDPE Geomembranes. J. Geotech. Geoenviron. Eng. 1997, 123, 57–65, doi:10.1061/(ASCE)1090-0241(1997)123:1(57).
8. O.D. Sherby, J.E. Dorn, Anelastic Creep of Polymethyl Methacrylate. Journal of the Mechanics and Physics of Solids 1958, 6, 145–162, doi:10.1016/0022-5096(58)90022-X.
9. L. Wang, W. Cen, E. Bauer, J. Wei, Z. Wen, J. Yan, Creep Failure Characteristics and Mathematical Modeling of High-Density Polyethylene Geomembranes under High Stress Levels. *Polymers* 2024, *16*, 2019, doi:10.3390/polym16142019.